Carboxylic acids from limonene oxidation by ozone and OH radicals: Insights into mechanisms derived using a FIGAERO-CIMS

Julia Hammes[1], Anna Lutz[1], Thomas Mentel[1,2], Cameron Faxon[1], and Mattias Hallquist[1]

[1]Department of Chemistry and Molecular Biology, University of Gothenburg, Gothenburg, Sweden
[2]Institute of Energy and Climate Research, IEK-8: Troposphere, Forschungszentrum Jülich GmbH, Jülich, Germany

Correspondence: Julia Hammes (julia.hammes@gu.se)

Abstract. This work presents the results from flow reactor studies on the formation of carboxylic acids from limonene oxidation under various conditions. A High Resolution Time Of Flight acetate Chemical Ionisation Mass Spectrometer (HR – TOF – CIMS) was used in combination with the Filter Inlet for Gases and AEROsols (FIGAERO) to measure the carboxylic acid profile in the gas and particle phases. The results revealed that limonene oxidation produced large amounts of carboxylic acids which are important contributors to secondary organic aerosol (SOA) formation. The highest 10 acids contributed 56–91% to the total gas-phase signal and the dominant gas-phase species in most experiments were $C_8H_{12}O_4$, $C_9H_{14}O_4$, $C_7H_{10}O_4$ and $C_{10}H_{16}O_3$. The particle-phase composition was generally more complex than the gas-phase composition and the highest 10 acids contributed 47–92% to the total signal. The dominant species in the particle phase were $C_8H_{12}O_5$, $C_9H_{14}O_5$, $C_9H_{12}O_5$ and $C_{10}H_{16}O_4$. The measured concentrations of dimers in the particle phase were very low, indicating that acidic dimers play a minor role in SOA formation via ozone/OH oxidation of limonene. Spearman correlation analysis of the produced carboxylic acid species and experimental parameters were helpful in interpreting the results. Based on the various experimental conditions, the acidic composition for all experiments were modelled using the Master Chemical Mechanisms (MCM). Significant concentrations of 11 acids, from a total of 16 acids, included in MCM were measured with the CIMS. However, the model predictions were, in some cases, inconsistent with the measurement results, especially in the case of the OH dependence. Reaction mechanisms are suggested to fill-in the knowledge gaps. Based on the mechanisms proposed in this work, nearly 75% of the qualitative gas-phase signal of the low concentration (ppb converted), humid, mixed oxidant experiment can be explained.

1 Introduction

Atmospheric aerosol particles have an impact on climate and human health and the respective effects depend on particle properties, number, size and chemical composition (Hallquist et al., 2009). Of the many constituents of atmospheric aerosol particles, organic aerosol particles are the least understood. Secondary organic aerosol (SOA) is the major component of organic aerosols. Identifying the chemical pathways of condensable products is essential for predicting SOA formation. However, this identification is inherently difficult as such products often reside in both the gas and particulate phases and continuous partitioning occurs between these two phases. Low vapour pressure products from radical- (i.e. OH) initiated oxidation or

ozonolysis of volatile organic compounds (VOCs), such as monoterpenes ($C_{10}H_{16}$), contribute significantly to atmospheric aerosol particle formation and growth (Hallquist et al., 2009). Limonene, the main constituent of the essential oil from citrus plants, is a widely used chemical in personal care and household-related consumer products (owing to its pleasant smell) and elevated indoor concentrations can be expected (Brown et al., 1994; Langer et al., 2008). The emission rates of limonene are

5   lower than those of other monoterpenes (e.g. α - pinene), and limonene is doubly unsaturated and exhibits high reactivity in the presence of ozone. Limonene has two chemically different double bonds, an endocyclic and an exocyclic double bond. The initial reaction will occur predominantly at the endocyclic double bond. However, the primary products may be unsaturated and exhibit high reactivity for further oxidation. The oxidation of limonene will eventually lead to the formation of SOA in both the atmosphere and indoor environments. The oxidation of monoterpenes and, specifically, limonene has been previously reported

10   (Leungsakul et al., 2005a, b; Walser et al., 2008; Maksymiuk et al., 2009) and basic reaction mechanisms that describe first- and second-generation oxidation products have been proposed. Due to their low vapour pressure, carboxylic acids, a major class of limonene-oxidation products can play an important role in SOA formation (Salo et al., 2010). The relative contribution of carboxylic acids from limonene oxidation to SOA formation has been assessed via a model (Pathak et al., 2012). According to that study, limonene-ozonolysis produces significant amounts of carboxylic acids and the distribution of these acids is affected

15   by the OH and ozone concentrations. During ozonolysis, limonene is attacked by ozone and forms an unstable and energy-rich primary ozonide (POZ), see fig. 1. The POZ will undergo decomposition where each oxygen contributes to the formation of a carbonyl and a carbonyl oxide group, the so-called excited Criegee intermediate (CI*). The 10 carbon skeleton is retained during this process. The CI* has a planar structure and the orientation of the outer oxygen will determine its chemical fate. The dominant reaction pathway (86% (Atkinson et al., 1992)) for limonene syn − CI* is the vinyl hydroperoxide channel

20   (VHP) which generates an alkyl radical under loss of an OH radical. This pathway provides a source for night-time OH in the atmosphere. The VHP requires an alkyl group in the syn position and is, hence, inaccessible to anti − CI*. The dominant fate of the anti − CI* is decomposition via the ester or the "hot acid" channel where an energy-rich ester or acid formed will undergo decomposition thereby resulting in various products. Two possible products, i.e. OH and an acyl radical (RC(O)•) (Vereecken and Francisco, 2012), which can react with O_2 and subsequently HO_2 to form a carboxylic acid and ozone. Furthermore, the

25   CI* can, to some extent, become collisionally stabilised (sCI) and exocyclic CI* are stabilised more efficiently than endocyclic CI*. The formed sCI will undergo further reactions and the reaction sCI + water will produce a carbonyl, an alkyl or an alkoxy radical. If the sCI contains an α - hydrogen, a carboxylic acid can be produced directly from the water reaction. Although the sCI + water reaction is likely the most dominant in the atmosphere, sCI may also react with carboxylic acids forming stable adducts which have been identified as dimer esters (Kristensen et al., 2016). The fate of RO_2 radicals in the absence of NO_x

30   includes a self-reaction ((R1 - R3), isomerisation via an internal H-shift (R4), and a reaction with HO_2 (R5) (Ehn et al., 2014). If RO_2 is an acylperoxy radical, a carboxylic acid can be formed.

$$RO_2 \bullet + RO_2 \bullet \rightarrow RO \bullet + O_2 \tag{R1}$$

Atmospheric
Chemistry
and Physics
Discussions

$$\rightarrow ROH + RCHO + O_2 \tag{R2}$$

$$\rightarrow ROOR + O_2 \tag{R3}$$

5

$$RO_2 \bullet [internal H-shift] \rightarrow \bullet ROOH \tag{R4}$$

$$RC(O)O_2 \bullet + HO_2 \bullet \rightarrow RC(O)OH + O_3 \tag{R5}$$

These reactions lead to further functionalisation, e.g. formation of acids, alcohols, carbonyls or peroxides and may in addition

10 produce alkoxy radicals. Subsequently, alkoxy radicals can be converted by oxygen to a carbonyl, if an α - hydrogen is present. Alkoxy radicals that lack this hydrogen will undergo isomerisation or decomposition via β - scission. During ozonolysis experiments, OH radicals are produced and react with the precursor as well as the reaction products. This process occurs in the laboratory as well as in the actual atmosphere and increases the complexity of the degradation mechanisms. In the laboratory, one can scavenge the produced OH radicals by adding a compound, e.g. 2-butanol, that reacts rapidly with OH, thereby

15 reducing OH. The OH scavenger reduces the OH concentration but leads to an increase in the HO_2 concentration. This yields changes in the distribution of radicals and subsequently the radical-dependent chemistry (Keywood et al., 2004). For example, the reaction of 2-butanol with OH produces HO_2 radicals with a yield of 64% (MCM v 3.3.1) thereby increasing the HO_2/RO_2 ratio. In laboratory experiments, these features can be employed in investigating the importance of various radicals/pathways for product distribution and subsequent SOA formation. The Gothenburg Flow Reactor for Oxidation Studies at Low Temperatures

20 (G-FROST) has been used in previous studies (Jonsson et al., 2006, 2008a, b; Kristensen et al., 2016; Faxon et al., 2017) to investigate the dependence of aerosol properties on different parameters (e.g. humidity and radical conditions). The G-FROST setup has now been extended with a High-Resolution Time-of-Flight Chemical Ionization Mass Spectrometer (HR-ToF-CIMS) that will provide insight into the chemical composition of the gas and particle phase through connection to the Filter Inlet for Gases and AEROsols (FIGAERO). These new techniques allow for sensitive simultaneous detection in the gas and particle

25 phases. Herein, an ionisation using acetate allows investigation of carboxylic acid formation. In the following, we analyse the carboxylic acid product spectrum of limonene. The goal is to detect major pathways and to compare the results with existing mechanisms, primarily developed for gas-phase chemistry related to the impact on tropospheric ozone formation, but now frequently used as a link to particle formation. This work (i) considers (for various limonene concentrations) the effect of humidity, OH scavenging and ozone level on carboxylic acid formation, and (ii) provides an outlook and suggestions for

30 mechanistic gaps with the aim of eventually describing major acidic products found in the gas and particle phases under realistic atmospheric conditions (i.e. ozonolysis is performed in the absence of an OH scavenger under low concentration and humidity conditions).

2 Materials and methods

Oxidation studies of limonene in the presence of ozone have been performed under a variety of experimental conditions (see table S1). The G-FROST system employed has been described in detail elsewhere (Jonsson et al., 2008a, b) and will only be presented briefly here. G-FROST consists of a laminar-flow reactor (vertical Pyrex glass cylinder, length 191 cm, inner diameter 10 cm, with a halocarbon wax coating) in a temperature-controlled housing (see fig. S1). The total inflow into the system was 1.6 LPM and the sample outflow was 0.94 LPM, yielding an average residence time of 240 s. The aerosol was sampled with a funnel system from the centre part of the laminar flow, to minimise wall effects. Limonene (Alfa Aesar, (R)-(+)-Limonene, 97%) was added by passing synthetic air (Laboratory Zero Air Generator, N-GC-6000, Linde Gas) through a characteristic diffusion source. Limonene was then pre-mixed with a dry or humidified bulk flow, with or without 2-butanol (Merck, p.a. >99%) as an OH scavenger. During each experiment, limonene concentrations were increased stepwise (15, 40, 150 ppb), while the temperature inside G-FROST was kept constant at 20°C for either dry (relative humidity (RH) <2%) or 40% RH conditions. Ozone (400, 1000, 5000 ppb) was generated by passing oxygen gas through a set of Pen-Ray® mercury lamps (UVP, λ 254 nm) and added through a separate 6mm Teflon line to G-FROST. The ozone level was kept constant during each experimental run. A summary of experimental conditions is provided in. The product distribution in the gas and particle phases was analysed with an acetate HR-ToF-CIMS (Aerodyne) (Bertram et al., 2011) coupled to the FIGAERO inlet (Lopez-Hilfiker et al., 2014). The reagent ion acetate is especially susceptible to acidic organic compounds such as carboxylic acids. The sample flow from G-FROST was diluted with ultra-high purity (UHP) nitrogen gas and pumped at 2 × 4 LPM by two diaphragm pumps (KNF, N816.3KN.18) through the FIGAERO inlet. Perfluoroheptanoic acid (PFHA, Sigma Aldrich, 99%) was used as the internal mass calibration standard. The gas-phase chemistry was determined via 60 min measurements and particles were collected simultaneously on a 1 μm 24 mm Zefluor® PTFE filter (Pall Corp.). During desorption, the temperature was increased from 25°C to 200°C in 50 min (3.5°C min^{-1}) and kept constant at 200°C for 10 min. Subsequently, UHP nitrogen gas was bubbled (flow rate: 0.02 LPM) through acetic anhydride (Sigma Aldrich, puriss p.a. ≥ 99%) and diluted with a bulk flow of UHP nitrogen to 2.2 LPM. This flow was reduced to 2 LPM using a critical orifice (O'Keefe Controls Co) and passed through a commercial 210Po alpha emitter (NDR, P-2021) to produce acetate reagent ions. A Scanning Mobility Particle Sizer (SMPS; CPC 3775 and DMA 3081, TSI Inc.) was used to measure the particle size distribution. The mass of the produced aerosol was determined, assuming a particle density of 1.4 g cm^{-3} (Hallquist et al., 2009). The CIMS data were analysed using the Tofware package (Tofwerk/Aerodyne) for IGOR Pro (WaveMetrics). The data were acquired at 1 Hz and pre-averaged to 0.0167 Hz (1 min) for further analysis. To account for thermal decomposition (double or triple peaks in desorption profile), the average (four desorption cycles per reaction condition) FIGAERO desorption profiles (thermograms) were analysed in Python 3.6.0 using the NumPy (v 1.11.3), SciPy library (v 0.18.1) and pandas (v 0.19.2) packages. The exponentially modified Gaussian function (Foley and Dorsey, 1984) was used as a peak shape function for peak fitting of the thermograms (fig. S2). The area of the fitted peaks was calculated by integrating along the given axis using the composite trapezoidal rule. Spearman correlation plots were calculated to assess the correlation of each dominant acid with the respective response to changes in the experimental parameters. All experiments have been modelled utilizing the MCM (v3.3.1) (see table S1 for the initial conditions). The initial

Atmospheric
Chemistry
and Physics

Discussions

concentration of 2-butanol was set to 3×10^5 µg m^{-3} in the case of OH scavenger experiments (Pathak et al., 2012). Based on the calculations, the amount of reacted limonene was derived. The OH, HO$_2$ and RO$_2$ levels enabling calculation of the corresponding values integrated over a reaction time of 240 s were used in the spearman correlation analysis.

3 Results and Discussion

5   A total of 33 different experiments have been performed under various reaction conditions (table S1). The general effect of parameters on SOA formation concurs with our previous results, where (for e.g.) an increase in SOA formation with increasing RH was observed (Jonsson et al., 2006). In the following, we will characterise the distribution of gas- and particle-phase organic acid. Figure 2 shows an example of a mass spectrum from one of the experiments. Over 100 different molecular formulas for acids have been identified, far exceeding the number of acids reported in previous studies (Glasius et al., 2000; Leungsakul

10   et al., 2005a; Jaoui et al., 2005, 2006; Walser et al., 2008; Rossignol et al., 2012, 2013). Here we will focus on the analysis of acids with carbon numbers ranging from seven to ten (and the dimers formed from these acids). The contribution of each acid to the total signal is calculated and the highest 10 ion signals are selected from each experiment. This yields a total of 32 different molecular compositions, representing the greatest fraction (47%–91%) of the total signal. The fraction corresponding to the sum of identified ions to the total signal can reveal the diversity of the product distribution for each condition. A low

15   coverage indicates an experiment where several compounds with the same intensities are generated. In general, the particle-phase composition is more diverse than the gas-phase composition (fig. 3). The presence of water in the system also increases the diversity of the product distribution in both the gas and particle phases. Compared with lower ozone concentrations, higher concentrations generally yield larger product diversity, owing to greater possibility for exocyclic double-bond oxidation or unsaturated-acid oxidation that yields a wider variety of products (fig. S3 and S4). The OH reaction pathways are suppressed

20   in experiments with an OH scavenger and the oxidation can then occur only via ozonolysis. This apparently reduces the oxidation product diversity of the particle phase, consistent with the findings of Watne et al. (2017). In that study, the volatility of limonene SOA produced via ozonolysis only was found to be more homogeneous than that of limonene produced via other/additional processes. However, the product distribution of the gas phase obtained via ozonolysis only is more diverse than the distribution obtained via other/additional processes. Generally, the most important acids (averaged over all experiments)

25   are C$_7$H$_{10}$O$_3$, C$_7$H$_{10}$O$_4$ C$_8$H$_{12}$O$_4$, C$_8$H$_{12}$O$_5$, C$_9$H$_{14}$O$_4$, C$_9$H$_{14}$O$_5$, C$_{10}$H$_{16}$O$_3$ and C$_{10}$H$_{16}$O$_4$. These are compared with the overview (table S2) of previously reported carboxylic acids (C7–C10) resulting from limonene ozonolysis. The proposed structures of these acids are also shown. Ten of the previously reported acid formulas are found in this study while three acids, C$_7$H$_{10}$O$_6$, C$_8$H$_{12}$O$_6$ and C$_8$H$_{14}$O$_4$, lie outside the ten highest corresponding ions identified in any of our 33 experiments. Leungsakul et al. (2005a) and Walser et al. (2008) reported that C$_9$H$_{14}$O$_4$, and C$_{10}$H$_{16}$O$_3$ were the most and second-most

30   dominant particle-phase compounds, respectively. However, in our study, the more oxidised (compared with C$_9$H$_{14}$O$_4$, and C$_{10}$H$_{16}$O$_3$) C$_9$H$_{14}$O$_5$, and C$_{10}$H$_{16}$O$_4$ are the most dominant particle-phase compounds. Most of the previously reported molecular formulas are included in the master chemical mechanism (MCM, http://mcm.leeds.ac.uk/MCM/). The MCM was originally developed to provide accurate, robust and current information regarding the role of specific organic compounds

Atmospheric
Chemistry
and Physics
Discussions

in ground-level ozone formation, in relation to air-quality policy development in Europe. Over the years, MCM has been employed in studies linked to SOA formation (Jenkin, 2004), although this mechanism is still under development to capturing descriptions on the fraction of low-volatility and often very oxygenated fraction of VOCs (Barley et al., 2011). In the present study, we employ a wider range of experimental conditions (than the range of conditions typically considered) to further

5   assess the influence of different parameters on the formation of the observed carboxylic acid products. In fig. S4, we show the correlations, using Spearman ranking, for each of the 32 different molecular compositions representing the majority of the ion signals. The results for the eight most important acid formulas, i.e. $C_7H_{10}O_3$, $C_7H_{10}O_4$ $C_8H_{12}O_4$, $C_8H_{12}O_5$, $C_9H_{14}O_4$, $C_9H_{14}O_5$, $C_{10}H_{16}O_3$ and $C_{10}H_{16}O_4$, are presented and discussed. These are all oxidation products with mass ranging from 130 m/z to 250 m/z and are identified as carboxylic acids with carbon numbers $\geq$ 10. Based on other studies (Kristensen et al.,

10   2012, 2014, 2016; Witkowski and Gierczak, 2014; Mohr et al., 2017), dimer formation is expected. These dimers are expected to contribute significantly to the particle phase. For the particle-phase data, compounds with mass above 300 m/z are detected and are identified as dimer species with carbon numbers >10. These compounds occur only in the particle phase. However, the relative signals are significantly lower than those reported (e.g.) for dimer formation in a study on limonene with nitrate radicals (Faxon et al., 2017) or the ozonolysis of other terpenes such as α - pinene (Kristensen et al., 2016). In the present study

15   the identified products must be acids, since we apply CI using the acetate ion. We conclude that, although dimer formation may occur (in general), no important acidic dimers are formed in the system. Consequently, we will focus on the formation of the monomer acids.

Water effect. Generally, most of the 32 top ions have higher signals in humidity experiments than in other environments. The opposite is true for the 400 ppb ozonolysis-only (OH-scavenged) cases (gas and particle phases). For experiments with OH

20   scavenger, the importance of water is evidenced by the prominent formation of gas-phase $C_{10}H_{16}O_3$, $C_9H_{16}O_3$, $C_9H_{14}O_3$ and $C_8H_{14}O_3$ (fig. S3). The water dependence of these acids is less pronounced in the mixed oxidation cases (except for $C_8H_{14}O_3$), than in other cases, but water seems to be favourable for the formation of other acids, such as $C_8H_{10}O_{4-5}$ and $C_7H_{10}O_{2-3}$. In general, water enhances the formation of the particle-phase acids. This concurs with the findings of Jonsson et al. (Jonsson et al., 2006) who reported an increase in the SOA number and mass under humid conditions. The authors attributed

25   (i) this result to an increase in the number of low-volatility products with increasing water concentration during the ozonolysis of limonene, and (ii) the water effect on SOA formation to $C_{10}H_{16}O_3$ formation. For humidity experiments considered in the present study, we observe a considerable increase and a slight increase in the formation of gas-phase $C_{10}H_{16}O_3$ and particle-phase $C_{10}H_{16}O_3$, respectively. Assuming that the humidity effect on $C_{10}H_{16}O_3$ production is responsible for the SOA dependence on humidity, subsequent transformation of condensed material is required as the particulate phase is deficient

30   in $C_{10}H_{16}O_3$.

Radical effect. Consistent with previously reported results on the SOA mass (Jonsson et al., 2008a; Pathak et al., 2012), the intensities of most acids in the low- and medium-ozone cases are higher for experiments employing mixed oxidation than for experiments employing an OH scavenger. For low-ozone and low-VOC experiments, the scavenger-provided SOA mass decreases with 2-butanol addition, as previously reported (Jonsson et al., 2008a), although the effect observed here is

35   weaker than the effect reported in that work. However, for relatively high concentrations of limonene, the opposite effect is

observed, i.e. the SOA mass increases with the use of a scavenger. Notably, this effect occurs independently of the acid-intensity behaviour, and may have resulted from the fact that (i) the SOAs associated with mixed oxidation are quite volatile and (ii) increased oxidation in the presence of OH, rather than converting semi volatiles to low/extremely low volatiles, converts volatiles/intermediate volatiles to semi volatile species, as suggested by Pathak et al. (2012); these are then lost during the

5   dilution process. Another possibility is that changes in the chemistry affect nucleation, as indicated by a size-distribution shift to smaller sizes which (compared with larger sizes) are more susceptible to evaporative losses in the dilution step. Separation of these effects during the experiments is impossible and, hence, the SOA formation potential associated with mixed oxidation may have been underestimated in this study. Owing to the sufficiently low ozone levels employed in the low and medium experiments, OH has an influence on the reaction pathways. At the highest ozone level, however, the intensities of acids

10   associated with mixed oxidation are lower than those resulting from the use of an OH scavenger. To investigate the effect of radical chemistry on the reaction pathways leading to the observed carboxylic acids, the OH, HO_2 and RO_2 concentrations are calculated and integrated using MCM for each experiment (fig. S3). A comparison of the mixed oxidation cases reveals that the formation of most gas-phase acids (e.g. $C_{10}H_{16}O_3$, $C_9H_{14}O_4$ and $C_7H_{10}O_3$) decreases with increasing amount of OH radicals in the system. The HO_2/RO_2 ratio has only a small influence on the mixed oxidation. However, when an OH scavenger is used,

15   the amount of gas-phase products ($C_{10}H_{16}O_3$, $C_{10}H_{16}O_4$, $C_9H_{14}O_4$ and $C_8H_{14}O_3$) decreases considerably with increasing HO_2/RO_2. The general influence of OH on acid formation is most pronounced for experiments performed under dry conditions. Under these conditions, OH and HO_2/RO_2 have a significant effect on the formation of $C_{10}H_{16}O_3$, $C_9H_{14}O_3$ and $C_7H_{10}O_4$. For example, $C_{10}H_{16}O_3$ and $C_9H_{14}O_3$ formation increases with increasing OH and decreasing HO_2/RO_2. The opposite is true for $C_7H_{10}O_4$ formation which decreases with increasing OH and decreasing HO_2/RO_2.

20   **Effect of excess ozone.** Experiments with high ozone levels are performed to assess the effect of excess ozone on acidic oxidation products. The aim is to oxidise, with ozone, the remaining double bond of the produced unsaturated carboxylic acids. The results show that ozone has a distinct negative impact on $C_7H_{10}O_{2-3}$ in the pure ozonolysis cases (see fig. S4) and, hence, we conclude that those compounds are unsaturated. Furthermore, the levels of gas-phase $C_{10}H_{16}O_3$, $C_9H_{16}O_3$, $C_9H_{14}O_{3-4}$ and $C_8H_{14}O_3$ are positively correlated with ozone in the absence of OH. For $C_{10}H_{16}O_3$, this is surprising as this

25   compound is assumed to be limononic acid, an unsaturated compound. This positive correlation may have resulted from the fact that the production of $C_{10}H_{16}O_3$ dominates over the removal (via ozonolysis) of the remaining double bond. The correlation with ozone is negative for most acids in the presence of OH and is most pronounced for gas-phase $C_{10}H_{16}O_3$, $C_9H_{14}O_3$ and $C_8H_{12}O_3$. The negative ozone correlation observed for mixed oxidation cases considering $C_{10}H_{16}O_3$ and $C_9H_{14}O_3$ concurs with the modelling results of a previous study that assessed the influence of ozone on limonene oxidation (Pathak

30   et al., 2012). A positive (albeit slightly) correlation with ozone is observed only for particle-phase $C_8H_{14}O_3$. The acid-ozone correlation obtained for humid conditions differs significantly from that obtained for dry conditions. The negative acid-ozone correlation is quite pronounced in the dry experiment cases and becomes increasingly negative (in general) for acids with relatively low carbon numbers, a trend unique to these experiments. The level of $C_{10}H_{16}O_3$ (especially the particle-phase) is positively correlated with ozone levels in the dry experiments. Generally, the amount of gas-phase acids have a stronger

35   positive correlation with the limonene consumption (Δ limonene) under humid conditions compared to dry experiments. In

Atmospheric
Chemistry
and Physics
Discussions

the dry experiments, $C_{10}H_{16}O_5$ and $C_9H_{14}O_4$ are the only acids with a strong positive correlation to Δ limonene. Compared with the occurrence of gas-phase acids, the occurrence of particle-phase acids is (in general) more strongly correlated with Δ limonene.

    Model results and comparison with experiments. Model calculations with the MCM (MCMv3.3.1) have been performed
5 for all 33 experimental conditions, in order to calculate Δ limonene and radical concentrations as well as product distributions, based on the experimental conditions. The modelled OH levels decrease with the initial limonene concentration, except for the highest ozone cases. High-ozone experiments yield the highest OH dose. The model results show that the HO_2/RO_2 ratio in experiments employing the OH scavenger 2-butanol is approximately one order of magnitude higher than that of the mixed oxidant experiments. This higher ratio results from the HO_2 radicals generated by the reaction of 2-butanol with OH.
10 According to the model calculations, RO_2 levels are generally 10 times higher than HO_2 levels when 2-butanol is included in the model. The $HO_2 + RO_2$ reaction is rapid and the typical rate constant is one order of magnitude larger than that of the $RO_2 + RO_2$ self-reaction (Orlando and Tyndall, 2012). In the MCMv3.3.1, 25 closed-shell carboxylic acids with 16 different chemical formulas are included for limonene. We identify 11 of the 16 acids (table S3; see table S5 for the model results of the MCM species). $C_9H_{14}O_3$ and $C_9H_{14}O_4$ are the most dominant and second-most dominant acids in all 33 modelled
15 experiments. $C_{10}H_{16}O_3$ (LIMONONIC), formed by the reaction of sCI + water, is the only acid that exhibits an overall positive water dependence. The model calculations predict that water should also have a positive influence on KLIMONONIC and CO25C6CO2H. However, this influence is undetectable in our experiments, owing to the extremely low concentrations of these compounds and the stronger influence exerted on other compounds with the same molecular mass. The model predicts that, compared with the presence of water, the presence of OH radicals has a greater influence on the product distribution.
20 Most individual MCM species exert a strong positive OH-chemistry effect in the model, except for LIMONONIC ($C_{10}H_{16}O_3$), C823CO3H ($C_9H_{14}O_5$), C823OOH ($C_8H_{14}O_4$) and C825OOH ($C_8H_{12}O_5$). In all cases, the concentrations estimated with the model of the last three compounds are highest when the OH chemistry is "turned off" (2-butanol added in model). C82CO2H ($C_9H_{14}O_3$) is produced to a lesser extent under humid and high ozone and for the highest OH conditions. It was produced to a higher extent under medium and low ozone and for the medium and lowest OH conditions. In the presence of OH chemistry,
25 the LIMONONIC concentration is lower under humid conditions than under dry conditions. The presence of OH is essential for the formation of numerous compounds (see table S5) and yields significant concentration only in the absence of 2-butanol, i.e. the modelled concentrations are close to zero in the presence of 2-butanol. For example, C731CO2H, KLIMONIC and KLIMONONIC are formed by ozone attack on the limona ketone which, in the model, is formed by the initial OH attack on the exocyclic double bond of limonene. Owing to the presence of 2-butanol, this attack on the double bond is reduced thereby
30 minimizing the amount of products generated. The correlation results for the humid and dry cases show that C823CO3H, C823OOH and C825OOH are negatively correlated with OH levels in the model. The reaction with OH represents the only destruction pathway of the produced acids in the model (even if unsaturated). This negative correlation indicates that, as the OH levels increase, the OH-induced destruction of the respective acid dominates over acid production. However, the reactions of unsaturated acids with ozone are neglected by the MCM. The experimental results reveal that the four dominant compounds
35 are $C_8H_{12}O_4$, $C_8H_{12}O_5$, $C_9H_{14}O_4$ and $C_9H_{14}O_5$. However, $C_9H_{14}O_5$ which plays only a minor role in the experiments,

Atmospheric
Chemistry
and Physics
Discussions

represents the dominant compound in the modelling results. $C_8H_{12}O_4$ which contributes significantly to the experimental results, is characterised by medium-level contribution to the model. $C_8H_{12}O_4$ and $C_8H_{12}O_5$ exhibit a positive OH-dependence in the model consistent with the gas-phase results obtained for $C_8H_{12}O_4$ under humid low-ozone and all medium-ozone experiments. The estimated concentration of $C_8H_{12}O_5$ is lower in the presence of OH chemistry for most conditions except

5   for humid low ozone experiments. The model reveals a positive OH dependence and a negative OH dependence for $C_9H_{14}O_4$ and $C_9H_{14}O_5$, respectively. The behaviour of the $C_9H_{14}O_4$ gas phase concurs with the model results for low- and medium-ozone experiments. For the highest ozone-level experiments, the levels observed for mixed oxidation are lower than those observed for oxidation in the presence of an OH scavenger. The OH dependence of $C_9H_{14}O_5$ in the experimental results differs from the overall negative OH dependence of modelled $C_9H_{14}O_5$. In contrast to the model predictions, the C7 acids

10    $C_7H_{10}O_4$ and $C_7H_{12}O_3$ contribute significantly to the gas-phase results and exhibit only a weak OH dependency. The model predicts a weak OH dependence for $C_{10}H_{16}O_3$ which is in stark contrast to the strong dependence revealed by the experimental results. Overall, most acids exhibit a positive RH dependence in the medium-ozone and humid low-ozone cases, a behaviour that is lacking from the modelling results. However, consistent with the modelling results, water in the system increases the concentration of $C_{10}H_{16}O_3$ by a factor of two. This hold true for all cases, except for the highest ozone cases where the

15   concentrations observed in the experiments are higher than the values predicted for dry conditions. In conclusion, significant concentrations of 11 acids (from a total of 16) included in MCM are measured with the CIMS. The model predictions are, in some cases, inconsistent with the measurement results, with the most notable inconsistencies occurring for the OH dependence.

4   Mechanism Interpretation and Outlook

The formation and the dependence of the eight most prominent ions in the experiments are only partly explained by the

20   MCMv3.3.1 and reaction pathways that form compounds with the molecular formulas $C_7H_{10}O_3$ and $C_{10}H_{16}O_4$ are absent. In the following, we propose reaction pathways for explaining the formation of some ions not accounted for in the model and propose additional pathways for compounds already included in MCM. Examples include reactions of unsaturated acid products with ozone or the formation of C10 acyl radicals via the hot acid channel (see pathway A in fig. 11). The largest discrepancy between model and experimental results is observed for the formation of compounds, such as the group of C7

25   acids or ketolimononic, -limonic or -limonalic acid which are OH-dependent in the model but are OH-independent in the observations. The dominance of $C_9H_{14}O_4$ and positive correlation with ozone can be explained by the additional formation of ketolimononic acid via reaction pathways as seen in fig. 4. Here, ozone attacks the double bond of the primary product limononic acid thereby forming a CI. In the case of exocyclic CI, sCI can be formed directly and the remaining CI* are usually more effectively stabilised than endocyclic CI* and therefore a larger yield of sCI can be expected. The produced sCI can

30   produce ketolimononic acid via the water channel (see fig. 4). Ketolimonalic ($C_8H_{12}O_4$) and ketolimonic ($C_8H_{12}O_5$) acid may be formed via the reaction of limonalic (R2, $C_9H_{14}O_3$) and limonic acid (R3, $C_9H_{14}O_4$), respectively, with ozone. The formation of a vinyl hydro peroxide (VHP) and subsequent decomposition via OH elimination and oxygen addition to the alkyl radical yields an alkyl peroxy radical. The bimolecular reaction of the alkyl peroxy with other RO_2 can lead to an alkoxy

Atmospheric
Chemistry
and Physics
Discussions

Open Access
EGU

radical which then can form a carbonyl and HO_2 upon reacting with oxygen. This reaction chain may explain the formation of $C_9H_{12}O_5$ and $C_8H_{10}O_{5-6}$. The model predictions for cases with and without the scavenger differ only slightly but the reaction pathway involving OH is an important contributor to $C_{10}H_{16}O_3$ formation in the experiments. This becomes especially clear when dry experiments with/without OH (with no possibility for the water pathway) are compared. The pathway leading to

5   the formation of $C_{10}H_{16}O_3$ via the hot acid channel from the anti – CI* (see fig. 1) is also neglected by the model. The remaining double bond can also be attacked by OH which would lead to the formation of an alkyl radical and subsequent addition of O_2. The reaction pathways shown in fig. 5 lead to the observed acid formation and may explain the formation of $C_7H_{10}O_4$, $C_9H_{14}O_4$ and $C_9H_{14}O_5$. The produced alkoxy radical will probably follow pathway A which produces the most stable radical and subsequently $C_7H_{10}O_4$. This pathway involves two bimolecular steps and is positively correlated with RO_2

10   levels in the system. Saturated compounds, although non-reactive with ozone, are susceptible to secondary chemical reactions induced by OH. The fate of the saturated compounds will depend on the relative reactivity of different sites to OH, and may include the abstraction of the acidic hydrogen followed by splitting off of CO_2 ; the subsequent bimolecular reactions will produce $C_7H_{10}O_4$. This reaction competes with the abstraction of the tertiary hydrogen, but will lead to products that are inconsequential to the present experimental results. The formation of $C_{10}H_{16}O_4$ results from processes other than ozonolysis

15   or OH attack on the exocyclic double bond of an acid product due to the fragmentation of the produced POZ and excessively high resulting O numbers. $C_{10}H_{16}O_4$ may have resulted from the reaction of an acylperoxy radical with HO_2 (see fig. 1) and the formation of a peroxy acid. However, the pathway for $C_7H_{10}O_3$ formation remains unclear.

For the particle phase, $C_8H_{12}O_5$ and $C_9H_{14}O_5$ are the dominating compounds in most experiments performed in this study, whereas $C_{10}H_{16}O_3$ (a major gas-phase compound) represents only a minor contributor to this phase. $C_{10}H_{16}O_4$ is

20   excluded from MCM, but plays a role in the particle-phase results. The formation of $C_{10}H_{16}O_4$ is positively correlated with the presence of RO_2 and HO_2. $C_9H_{14}O_3$ and $C_9H_{14}O_4$ are the dominant acids in the model calculations, but are only minor compounds in the particle phase. $C_9H_{14}O_4$ formation seems to occur only in experiments with the highest limonene content. Rapid autoxidation for the formation of highly oxidised molecules (HOMs) has recently gained significant attention (Ehn et al., 2014). This autoxidation proceeds via intramolecular H abstraction of RO_2 and subsequent formation of hydroperoxide

25   groups. RO_2 lifetimes in low NO_x environments are usually sufficient for the occurrence of this process (Orlando and Tyndall, 2012). During this process, large amounts of oxygen are rapidly introduced into the molecules, leading to a decrease in their vapour pressure. Most of the RO_2 will originate from the VHP channel, in the case of limonene ozonolysis, and products will probably be non-identifiable unless the radical termination reaction yields a carboxylic acid. Even if the formed compounds contain one or more carboxylic acid groups, the corresponding low vapour pressure may be undetectable by the used FIGAERO

30   inlet. Jokinen et al. Jokinen et al. (2014) investigated the formation of HOM from limonene and found that highly oxygenated monomers (C10) and dimers (C20) with oxygen numbers ranging from 5 to 11 and 7 to 18, respectively, play a crucial role in this formation. Only one compound with the same chemical formula ($C_9H_{14}O_5$) has been found in this study but it is unclear if the chemical structure is the same. In this study, dimers have exclusively been detected in the particle phase and are absent from the gas phase, owing to their potentially low vapour pressure. The formation of dimer esters from α - pinene ozonolysis

35   has recently been investigated (Kristensen et al., 2016). In that work, the reaction of sCI with carboxylic acids, suggested as

the formation pathway in the gas phase, was followed by partitioning into the particle phase. Consequently, the carboxylic acid group is lost in the esterification process which may explain the relatively low signals observed for acidic dimers in the present study. A potential acidic dimer ester will only be detectable if the dimer has a carboxylic acid group, as in the case of a di or tri carboxylic acid, or if the sCI carries a carboxylic acid group. Unsaturated dimers may react with ozone. The

5 $C_{18}H_{28}O_8$, $C_{19}H_{30}O_7$ compounds can form via the reaction of the endocyclic limonene sCI with ketolimonic ($C_8H_{12}O_5$) or limonic ($C_9H_{14}O_4$) acid, respectively (see fig. 7). In addition, $C_{19}H_{30}O_8$ may be formed from the dimerization reaction of limononic acid and the limononic-sCI. Gas-phase dimerization reactions of dominating C7–C10 acids with sCI account for only some of the dimer formulas. Reactions of acids with relatively small carbon numbers (<C7), RO_2 dimerization reactions or condensed-phase reactions may account for the other formulas.

10 ## 5 Conclusions

Figure 8 A provides an overview of the most important acidic compounds found in this study. These are identified by comparing the average contribution of each compound to all 33 experiments. Explicit formation pathways for the compounds $C_{10}H_{16}O_4$ and $C_9H_{12}O_5$ implemented in the MCM and additional reaction pathways for $C_7H_{10}O_4$, $C_8H_{12}O_{4-5}$, $C_9H_{14}O_{4-5}$ and $C_{10}H_{16}O_3$ are proposed. Structures for $C_{10}H_{14}O_5$ and $C_{10}H_{16}O_4$ have been proposed in previous studies (Glasius et al.,

15 2000; Leungsakul et al., 2005a; Jaoui et al., 2006; Walser et al., 2008; Rossignol et al., 2012) but the current mechanistic understanding is inadequate for explaining the formation of compounds with the proposed structures. In fig. 8 A, we show that the mechanisms proposed in this work can improve the qualitative understanding of the formation characterising (on average) 65% of the dominant gas-phase compounds and 50% of the particle-phase compounds. Notably, the particle-phase data correspond partly to compounds with low oxygen content (2–3 Oxygen) and their formation and negative correlation with ozone

20 remain unclear and require further study. However, only a few acidic dimers are detected. This may have resulted from lack of evaporation of these dimers (i.e. as acidic dimers) or loss of the acid functional group from potential acid monomer precursors during the dimer formation, as suggested in previous studies (Witkowski and Gierczak, 2014; Kristensen et al., 2016; Wang et al., 2016). Experiment 1, performed at low concentrations, for mixed oxidants and under humid conditions, should best represent atmospheric conditions. The summarised signal of the highest 10 acids in experiment 1 can be qualitatively

25 attributed to 89% of the gas phase and the proposed mechanisms in this study account for 74% of the total signal (see fig. 8 B). The particle-phase composition can be qualitatively explained (by up to 42%) by the mechanisms proposed in this work. The relatively large percentage of unexplained signal in the atmospheric case will result in large uncertainties when the acidic-particle phase composition of limonene SOA is modelled based on existing mechanisms (e.g. MCM) and partitioning theory. For a more quantitative mechanism (compared with the mechanism considered), inclusion of non-acidic products is required

30 for a complete picture of the oxidation products. Furthermore, secondary and tertiary chemistry must be considered when the oxidation of compounds is modelled. Subsequent aerosol formation as well as dimerization and condensed-phase reactions must also be evaluated.

Atmospheric
Chemistry
and Physics
Discussions

Open Access

Data availability. The data set is available upon request by contacting Mattias Hallquist (hallq@chem.gu.se).

Competing interests. The authors declare that they have no competing interest.

Atmospheric
Chemistry
and Physics
Discussions

References

Atkinson, R., Aschmann, S. M., Arey, J., and Shorees, B.: Formation of OH radicals in the gas phase reactions of O3 with a series of terpenes, Journal of Geophysical Research, 97, https://doi.org/10.1029/92jd00062, 1992.

Barley, M. H., Topping, D., Lowe, D., Utembe, S., and McFiggans, G.: The sensitivity of secondary organic aerosol (SOA) component partitioning to the predictions of component properties - Part 3: Investigation of condensed compounds generated by a near-explicit model of VOC oxidation, Atmospheric Chemistry and Physics, 11, 13 145–13 159, https://doi.org/10.5194/acp-11-13145-2011, 2011.

Bertram, T. H., Kimmel, J. R., Crisp, T. A., Ryder, O. S., Yatavelli, R. L. N., Thornton, J. A., Cubison, M. J., Gonin, M., and Worsnop, D. R.: A field-deployable, chemical ionization time-of-flight mass spectrometer, Atmospheric Measurement Techniques, 4, 1471–1479, https://doi.org/10.5194/amt-4-1471-2011, 2011.

Brown, S. K., Sim, M. R., Abramson, M. J., and Gray, C. N.: Concentrations of Volatile Organic-Compounds in Indoor Air - a Review, Indoor Air-International Journal of Indoor Air Quality and Climate, 4, 123–134, https://doi.org/DOI 10.1111/j.1600-0668.1994.t01-2-00007.x, 1994.

Ehn, M., Thornton, J. A., Kleist, E., Sipila, M., Junninen, H., Pullinen, I., Springer, M., Rubach, F., Tillmann, R., Lee, B., Lopez-Hilfiker, F., Andres, S., Acir, I. H., Rissanen, M., Jokinen, T., Schobesberger, S., Kangasluoma, J., Kontkanen, J., Nieminen, T., Kurten, T., Nielsen, L. B., Jorgensen, S., Kjaergaard, H. G., Canagaratna, M., Maso, M. D., Berndt, T., Petaja, T., Wahner, A., Kerminen, V. M., Kulmala, M., Worsnop, D. R., Wildt, J., and Mentel, T. F.: A large source of low-volatility secondary organic aerosol, Nature, 506, 476–9, https://doi.org/10.1038/nature13032, 2014.

Faxon, C., Hammes, J., Pathak, R. K., and Hallquist, M.: Characterization of organic nitrate constituents of secondary organic aerosol (SOA) from nitrate-radical-initiated oxidation of limonene using High-Resolution Chemical Ionization Mass Spectrometry, Atmospheric Chemistry and Physics Discussions, pp. 1–25, https://doi.org/https://doi.org/10.5194/acp-2017-584, 2017.

Foley, J. P. and Dorsey, J. G.: A Review of the Exponentially Modified Gaussian (EMG) Function: Evaluation and Subsequent Calculation of Universal Data, Journal of Chromatographic Science, 22, 40–46, https://doi.org/10.1093/chromsci/22.1.40, 1984.

Glasius, M., Lahaniati, M., Calogirou, A., Di Bella, D., Jensen, N. R., Hjorth, J., Kotzias, D., and Larsen, B. R.: Carboxylic acids in secondary aerosols from oxidation of cyclic monoterpenes by ozone, Environ Sci Technol, 34, 1001–1010, https://doi.org/DOI 10.1021/es990445r, 2000.

Hallquist, M., Wenger, J. C., Baltensperger, U., Rudich, Y., Simpson, D., Claeys, M., Dommen, J., Donahue, N. M., George, C., Goldstein, A. H., Hamilton, J. F., Herrmann, H., Hoffmann, T., Iinuma, Y., Jang, M., Jenkin, M. E., Jimenez, J. L., Kiendler-Scharr, A., Maenhaut, W., McFiggans, G., Mentel, T. F., Monod, A., Prévôt, A. S. H., Seinfeld, J. H., Surratt, J. D., Szmigielski, R., and Wildt, J.: The formation, properties and impact of secondary organic aerosol: current and emerging issues, Atmospheric Chemistry and Physics, 9, 5155–5236, https://doi.org/10.5194/acp-9-5155-2009, 2009.

Jaoui, M., Kleindienst, T. E., Lewandowski, M., Offenberg, J. H., and Edney, E. O.: Identification and quantification of aerosol polar oxygenated compounds bearing carboxylic or hydroxyl groups. 2. Organic tracer compounds from monoterpenes, Environ Sci Technol, 39, 5661–5673, https://doi.org/10.1021/es048111b, 2005.

Jaoui, M., Corse, E., Kleindienst, T. E., Offenberg, J. H., Lewandowski, M., and Edney, E. O.: Analysis of Secondary Organic Aerosol Compounds from the Photooxidation ofd-Limonene in the Presence of NOXand their Detection in Ambient PM2.5, Environ Sci Technol, 40, 3819–3828, https://doi.org/10.1021/es052566z, 2006.

Jenkin, M. E.: Modelling the formation and composition of secondary organic aerosol from a- and b-pinene ozonolysis using MCM v3, Atmospheric Chemistry and Physics, 4, 1741–1757, https://doi.org/10.5194/acp-4-1741-2004, 2004.

Jokinen, T., Sipila, M., Richters, S., Kerminen, V. M., Paasonen, P., Stratmann, F., Worsnop, D., Kulmala, M., Ehn, M., Herrmann, H., and Berndt, T.: Rapid autoxidation forms highly oxidized RO2 radicals in the atmosphere, Angew Chem Int Ed Engl, 53, 14 596–600, https://doi.org/10.1002/anie.201408566, 2014.

Jonsson, s., Hallquist, M., and Ljungström, E.: Impact of Humidity on the Ozone Initiated Oxidation of Limonene, delta3-Carene, and a-Pinene, Environ Sci Technol, 40, 188 – 194, https://doi.org/S0013-936X(05)01163-6, 2006.

Jonsson, s., Hallquist, M., and Ljungström, E.: The effect of temperature and water on secondary organic aerosol formation from ozonolysis of limonene, delta3-carene and a-pinene, Atmospheric Chemistry and Physics, 8, 6541–6549, https://doi.org/10.5194/acp-8-6541-2008, 2008a.

Jonsson, s., Hallquist, M., and Ljungstroöm, E.: Influence of OH Scavenger on the Water Effect on Secondary Organic Aerosol Formation from Ozonolysis of limonene, delta3-carene and a-pinene, Environ Sci Technol, 42, 5938–5944, https://doi.org/10.1021/es702508y, 2008b.

Keywood, M. D., Kroll, J. H., Varutbangkul, V., Bahreini, R., Flagan, R. C., and Seinfeld, J. H.: Secondary Organic Aerosol Formation from Cyclohexene Ozonolysis: Effect of OH Scavenger and the Role of Radical Chemistry, Environ Sci Technol, 38, 3343–3350, https://doi.org/10.1021/es049725j, 2004.

Kristensen, K., Enggrob, K. L., King, S. M., Worton, D. R., Platt, S. M., Mortensen, R., Rosenoern, T., Surratt, J. D., Bilde, M., Goldstein, A. H., and Glasius, M.: Formation and occurrence of dimer esters of pinene oxidation products in atmospheric aerosols, Atmospheric Chemistry and Physics Discussions, 12, 22 103–22 137, https://doi.org/10.5194/acpd-12-22103-2012, 2012.

Kristensen, K., Cui, T., Zhang, H., Gold, A., Glasius, M., and Surratt, J. D.: Dimers in a-pinene secondary organic aerosol: effect of hydroxyl radical, ozone, relative humidity and aerosol acidity, Atmospheric Chemistry and Physics, 14, 4201–4218, https://doi.org/10.5194/acp-14-4201-2014, 2014.

Kristensen, K., Watne, g. K., Hammes, J., Lutz, A., Petäjä, T., Hallquist, M., Bilde, M., and Glasius, M.: High-Molecular Weight Dimer Esters Are Major Products in Aerosols from a-Pinene Ozonolysis and the Boreal Forest, Environ Sci Technol, 3, 280–285, https://doi.org/10.1021/acs.estlett.6b00152, 2016.

Langer, S., Moldanova, J., Arrhenius, K., Ljungstrom, E., and Ekberg, L.: Ultrafine particles produced by ozone/limonene reactions in indoor air under low/closed ventilation conditions, Atmospheric Environment, 42, 4149–4159, https://doi.org/10.1016/j.atmosenv.2008.01.034, 2008.

Leungsakul, S., Jaoui, M., and Kamens, R. M.: Kinetic mechanism for predicting secondary organic aerosol formation from the reaction of d-limonene with ozone, Environ Sci Technol, 39, 9583–94, 2005a.

Leungsakul, S., Jeffries, H. E., and Kamens, R. M.: A kinetic mechanism for predicting secondary aerosol formation from the reactions of d-limonene in the presence of oxides of nitrogen and natural sunlight, Atmospheric Environment, 39, 7063–7082, https://doi.org/10.1016/j.atmosenv.2005.08.024, 2005b.

Lopez-Hilfiker, F. D., Mohr, C., Ehn, M., Rubach, F., Kleist, E., Wildt, J., Mentel, T. F., Lutz, A., Hallquist, M., Worsnop, D., and Thornton, J. A.: A novel method for online analysis of gas and particle composition: description and evaluation of a Filter Inlet for Gases and AEROsols (FIGAERO), Atmospheric Measurement Techniques, 7, 983–1001, https://doi.org/10.5194/amt-7-983-2014, 2014.

Maksymiuk, C. S., Gayahtri, C., Gil, R. R., and Donahue, N. M.: Secondary organic aerosol formation from multiphase oxidation of limonene by ozone: mechanistic constraints via two-dimensional heteronuclear NMR spectroscopy, Phys Chem Chem Phys, 11, 7810–8, https://doi.org/10.1039/b820005j, 2009.

Mohr, C., Lopez-Hilfiker, F. D., Yli-Juuti, T., Heitto, A., Lutz, A., Hallquist, M., D'Ambro, E. L., Rissanen, M. P., Hao, L. Q., Schobes-
5   berger, S., Kulmala, M., Mauldin, R. L., Makkonen, U., Sipila, M., Petaja, T., and Thornton, J. A.: Ambient observations of dimers from terpene oxidation in the gas phase: Implications for new particle formation and growth, Geophysical Research Letters, 44, 2958–2966, https://doi.org/10.1002/2017gl072718, 2017.

Orlando, J. J. and Tyndall, G. S.: Laboratory studies of organic peroxy radical chemistry: an overview with emphasis on recent issues of atmospheric significance, Chem Soc Rev, 41, 6294–317, https://doi.org/10.1039/c2cs35166h, 2012.

10   Pathak, R. K., Salo, K., Emanuelsson, E. U., Cai, C., Lutz, A., Hallquist, A. M., and Hallquist, M.: Influence of ozone and radical chemistry on limonene organic aerosol production and thermal characteristics, Environ Sci Technol, 46, 11 660–9, https://doi.org/10.1021/es301750r, 2012.

Rossignol, S., Chiappini, L., Perraudin, E., Rio, C., Fable, S., Valorso, R., and Doussin, J. F.: Development of a parallel sampling and analysis method for the elucidation of gas/particle partitioning of oxygenated semi-volatile organics: a limonene ozonolysis study, Atmospheric
15   Measurement Techniques, 5, 1459–1489, https://doi.org/10.5194/amt-5-1459-2012, 2012.

Rossignol, S., Rio, C., Ustache, A., Fable, S., Nicolle, J., Meme, A., D'Anna, B., Nicolas, M., Leoz, E., and Chiappini, L.: The use of a housecleaning product in an indoor environment leading to oxygenated polar compounds and SOA formation: Gas and particulate phase chemical characterization, Atmospheric Environment, 75, 196–205, https://doi.org/10.1016/j.atmosenv.2013.03.045, 2013.

Salo, K., Jonsson, A. M., Andersson, P. U., and Hallquist, M.: Aerosol volatility and enthalpy of sublimation of carboxylic acids, J Phys
20   Chem A, 114, 4586–94, https://doi.org/10.1021/jp910105h, 2010.

Vereecken, L. and Francisco, J. S.: Theoretical studies of atmospheric reaction mechanisms in the troposphere, Chem Soc Rev, 41, 6259–93, https://doi.org/10.1039/c2cs35070j, 2012.

Walser, M. L., Desyaterik, Y., Laskin, J., Laskin, A., and Nizkorodov, S. A.: High-resolution mass spectrometric analysis of secondary organic aerosol produced by ozonation of limonene, Phys Chem Chem Phys, 10, 1009–22, https://doi.org/10.1039/b712620d, 2008.

25   Wang, M., Yao, L., Zheng, J., Wang, X., Chen, J., Yang, X., Worsnop, D. R., Donahue, N. M., and Wang, L.: Reactions of Atmospheric Particulate Stabilized Criegee Intermediates Lead to High-Molecular-Weight Aerosol Components, Environ Sci Technol, 50, 5702–10, https://doi.org/10.1021/acs.est.6b02114, 2016.

Watne, A. K., Westerlund, J., Hallquist, A. M., Brune, W. H., and Hallquist, M.: Ozone and OH-induced oxidation of monoter-penes: Changes in the thermal properties of secondary organic aerosol (SOA), Journal of Aerosol Science, 114, 31–41,
30   https://doi.org/10.1016/j.jaerosci.2017.08.011, 2017.

Witkowski, B. and Gierczak, T.: Early stage composition of SOA produced by a-pinene/ozone reaction: a-Acyloxyhydroperoxy aldehydes and acidic dimers, Atmospheric Environment, 95, 59–70, https://doi.org/10.1016/j.atmosenv.2014.06.018, 2014.
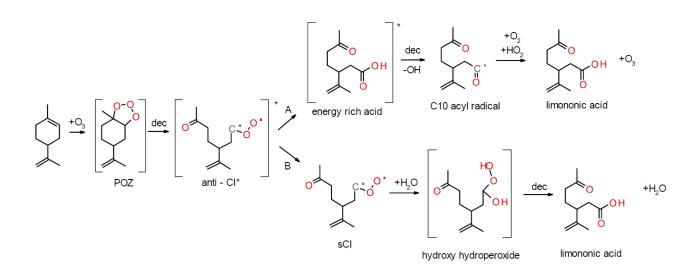
Figure 1. (A) Example of initial reactions of limonene with ozone to form limononic acid from the anti – CI* via the hot acid channel and (B) the collisional stabilisation channel (Vereecken and Francisco, 2012).
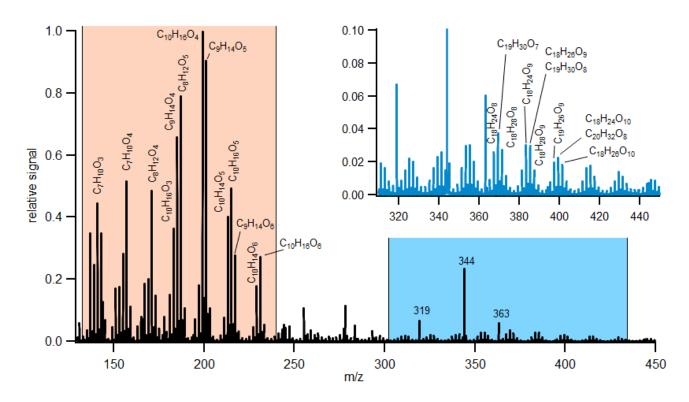
Figure 2. Example MS for medium-ozone and high-limonene conditions with OH-S for particle-phase data with identified monomers (orange region) and selected dimers (blue region). The peaks at 319, 344 and 363 are associated with the mass calibrant PFHA.
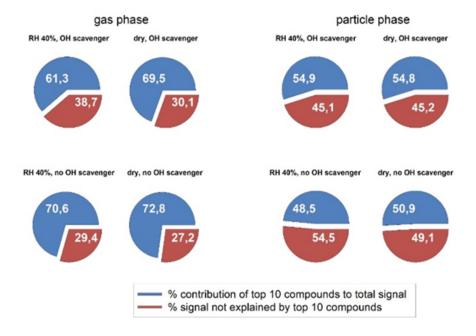
Figure 3. Explained and unexplained fractions of gas and particle phases for selected experiments with 1000 ppb ozone and 150 ppb limonene.

Figure 4. Proposed reaction mechanisms for secondary ozone chemistry of limononic (R1), limonic (R2) and limonalic (R3) acid.
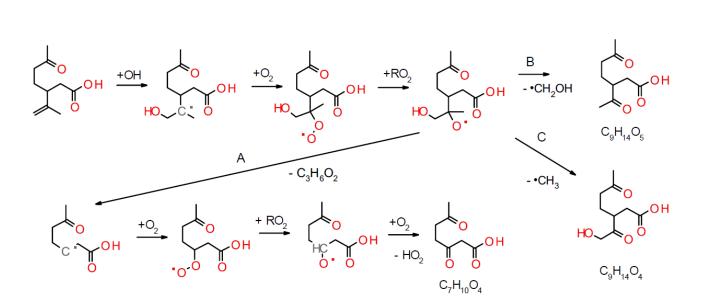
Figure 5. Addition of OH to the remaining unsaturated double bond of limononic acid and formation of $C_7H_{10}O_4$, $C_9H_{14}O_4$ and $C_9H_{14}O_5$.
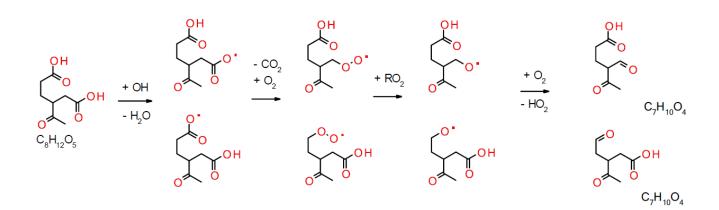
Figure 6. Secondary chemistry of selected saturated carboxylic acid product.
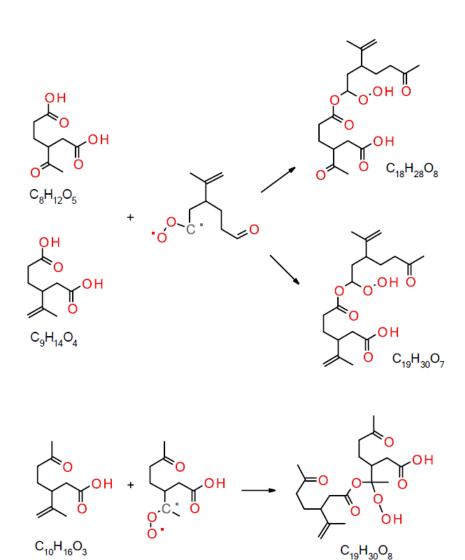
Figure 7. Proposed formation of $C_{18}H_{28}O_8$, $C_{19}H_{30}O_7$ and $C_{19}H_{30}O_8$.

Atmospheric
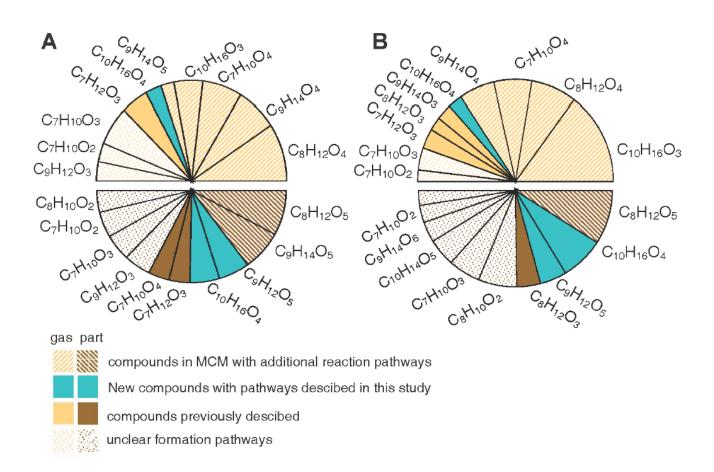Chemistry
and Physics

Open Access

EGU

Discussions

Figure 8. (A) Averaged 10 highest contributors to all experiments. (B) Highest 10 contributors to experiment 1. Pie charts showing the percentage contribution of each compound to the top 10. Top half wheel shows the gas-phase data and the bottom wheel shows the particle-phase data.